

Full counting statistics of transport through two-channel Coulomb blockade systems

Shi-Kuan Wang, Hujun Jiao, Feng Li, and Xin-Qi Li*
*State Key Laboratory for Superlattices and Microstructures, Institute of Semiconductors,
 Chinese Academy of Sciences, P.O. Box 912, Beijing 100083, China*

YiJing Yan

Department of Chemistry, Hong Kong University of Science and Technology, Kowloon, Hong Kong
 (Dated: February 8, 2020)

A mesoscopic Coulomb blockade system with two identical transport channels is studied in terms of full counting statistics. It is found that the average current cannot distinguish the quantum constructive interference from the classical non-interference, but the shot noise and skewness are more sensitive to the nature of quantum mechanical interference and can fulfill that task. The interesting super-Poisson shot noise is found and is demonstrated as a consequence of constructive interference, which induces an effective system with fast-and-slow transport channels. Dephasing effects on the counting statistics are carried out to display the continuous transition from quantum interfering to non-interfering transports.

Rather than average current, the current fluctuations in mesoscopic transport can sometimes provide deep insight into the nature of transport mechanisms [1]. A fascinating theoretical approach, known as full counting statistics (FCS) theory [2, 3], can simultaneously yield all the statistical cumulants of the number of transferred charges (i.e., all zero-frequency current-correlation functions). Experimentally, the real-time counting statistics has been carried out in transport through quantum dots [4], representing a crucial achievement of being able to count individual electron tunnel events.

For charge transport at very low transmission, the uncorrelated transmission events are Poisson processes. However, the Fermi-Dirac statistics together with the possible many-body Coulomb interaction usually enhances correlation among the transport electrons, and thereby results in sub-Poisson noise [5]. It is thus of interest to examine mechanisms that can lead to super-Poisson-noise behavior, since the current fluctuations can be used in reverse to gain insight into the nature of unusual transport mechanisms. The mechanisms proposed so far for the super-Poisson noise include such as double electron charge transfer by Andreev reflection in normal-superconductor (NS) junction [6, 7], multiple electron charge transfer by multiple Andreev reflections in SNS system [8, 9, 10, 11], dynamical channel blockade [12, 13, 14], dynamical spin blockade [15], bistability [16], cotunneling [17, 18], electron-phonon interaction in shuttle system [19], and decoherence in mesoscopic coherent population trapping system [20].

In this work we consider a relatively simple system, say, electronic transport through a Coulomb blockade system with two identical transport channels, which can be realized experimentally by transport through two adjacent levels in a single quantum dot (QD) [21], or through two QDs in parallel [22, 23]. This type of setup itself is of

particular interest, since it is an analogue of the optical double-slit interferometer. In this context the underlying quantum interference and phase accumulations through QDs have been the subjects of intensive studies [24, 25, 26]. Our present study will be placed at the level of FCS, from which a number of interesting effects of quantum interference on current fluctuations will be revealed.

Model Description

The transport through a two-channel Coulomb blockade system is governed by the Hamiltonian

$$H = H_D + H_{Leads} + H_T, \quad (1a)$$

$$H_D = E_1 d_1^\dagger d_1 + E_2 d_2^\dagger d_2 + U n_1 n_2, \quad (1b)$$

$$H_{Leads} = \sum_k (\varepsilon_{Lk} c_{Lk}^\dagger c_{Lk} + \varepsilon_{Rk} c_{Rk}^\dagger c_{Rk}), \quad (1c)$$

$$H_T = \sum_{jk} [\Omega_{jL} d_j^\dagger c_{Lk} + \Omega_{jR} d_j^\dagger c_{Rk} + \text{H.c.}]$$

Here $c_{Lk, Rk}^\dagger (c_{Lk, Rk})$ and $d_j^\dagger (d_j)$ are the electron creation (annihilation) operators, for the electrode reservoirs and central dot states, respectively. The two channels are characterized by states with energy levels E_1 and E_2 . Couplings of these two dot states to the electrodes are described by $\Omega_{jL(R)}$, or $\Gamma_{L,R}^j = 2\pi g_{L,R} |\Omega_{jL,jR}|^2$, for latter use. Here $g_{L,R}$ are the density of states (DOS) of the electron reservoirs. To manifest maximally the quantum interference effect, we shall focus on two *identical* transmission paths. This can be accomplished by assuming equal and energy independent coupling strengths of the two dot states with the left and right electrodes, i.e., $|\Omega_{1L(R)}| = |\Omega_{2L(R)}| = \Omega_{L(R)}$, and $\Gamma_{L(R)}^1 = \Gamma_{L(R)}^2 = \Gamma_{L(R)}$. To address the quantum interference between transmissions through the two channels, the relative phase difference is significant. Physically, the phase difference contains

*Electronic address: xqli@red.semi.ac.cn

the phase accumulation of spatial motion from the electrode to dot, particularly in the presence of magnetic vector potential (i.e., the Aharonov-Bohm effect), as well as the phase changes associated with transmission through quantum dots [25, 26]. Nevertheless, in this work we would like to adopt a phenomenological way to account for all these phase accumulations, by choosing $\Omega_{1L} = \Omega_{2L}$, and $\eta = \Omega_{1R}/\Omega_{2R}$. Here η can be regarded as a relative phase parameter. Note that the alternative gauge, say, $\Omega_{1R} = \Omega_{2R}$ and $\eta = \Omega_{1L}/\Omega_{2L}$, does not affect the final results [21]. In this paper, we also assumed $\eta = \pm 1$, i.e., only complete constructive and destructive interference are considered.

In the above Hamiltonian we omitted the spin indices, thus did not explicitly write out the on-site Coulomb interaction terms, and only left Un_1n_2 to describe Coulomb interaction between electrons in the different dot states. In this work, unless explicit specification, our study will be restricted to the strong Coulomb blockade regime, which only allows for three available occupation states, i.e., $|0\rangle$, $|1\rangle$, and $|2\rangle$, corresponding to, respectively, empty dot state, and states with one electron on either E_1 or E_2 .

FCS Formulation

Before going to the specific study of the above described system, we would like first to reformulate the FCS formalism based on the particle-number-resolved master equation approach [27, 28, 29, 30]. As pointed out in Ref. 31, the pioneering work [2, 3] and a few other approaches developed latter [10, 32, 33] are largely restricted to addressing the FCS of noninteracting electrons. While Ref. 31 developed an elegant theory of FCS for mesoscopic systems in strong Coulomb blockade limit, however the system's internal *quantum coherence* did not enter it since the theory was constructed on the basis of classical stochastic processes. It is thus advantageous to formulate an approach of being able to account for both the internal quantum coherence and the many-body Coulomb interaction on equal footing. Although such type of approach has been described and applied to coherent and interacting systems [34, 35], for completeness we would like here to reformulate it, hopefully in a more transparent and unified way.

To relate with our earlier work [29, 30], we rename $H_S \equiv H_D$, $H_B \equiv H_{Leads}$, and reexpress $H' \equiv H_T$ as

$$H' = H_T = \sum_{j=1}^2 [d_j^\dagger F_j + \text{H.c.}], \quad (2a)$$

$$F_j = \sum_k \Omega_{jL} c_{Lk} + \sum_k \Omega_{jR} c_{Rk} = f_{Lj} + f_{Rj}. \quad (2b)$$

Regarding H' as perturbation, the second-order cumulant expansion leads to a formal master equation for the

system's reduced density matrix [29, 30]:

$$\dot{\rho}(t) = -i\mathcal{L}\rho(t) - \int_0^t d\tau \langle \mathcal{L}'(t)\mathcal{G}(t,\tau)\mathcal{L}'(\tau)\mathcal{G}^\dagger(t,\tau) \rangle \rho(t). \quad (3)$$

Here the Liouvillian superoperators are defined as $\mathcal{L}\rho = [H_S, \rho]$, $\mathcal{L}'\rho = [H', \rho]$, and $\mathcal{G}(t,\tau)(...) = G(t,\tau)(...)G^\dagger(t,\tau)$, with $G(t,\tau)$ the usual propagator associated with system Hamiltonian H_S . The reduced density matrix $\rho(t) = \text{Tr}_B[\rho_T(t)]$, and $\langle \dots \rangle = \text{Tr}_B[\dots \rho_B]$ with ρ_B the density matrix of the electron reservoirs.

The trace in Eq.(3) is over all the electrode degrees of freedom. To achieve the FCS of current fluctuations, we would like to keep track of the records of electron numbers emitted from the source lead (n_1) and arrived at the drain lead (n_2). We therefore classify the Hilbert space of the reservoirs as follows: $B^{(n_1, n_2)} = B_L^{(n_1)} \otimes B_R^{(n_2)}$. The entire Hilbert space of electron reservoirs is thus decomposed as $B = \bigoplus_{n_1, n_2} B^{(n_1, n_2)}$.

With this classification the average over states in the entire bath Hilbert space in Eq. (3) is replaced with the average over states in the subspace $B^{(n_1, n_2)}$, leading to a conditional master equation

$$\dot{\rho}^{(n_1, n_2)}(t) = -i\mathcal{L}\rho^{(n_1, n_2)}(t) - \int_0^t d\tau \text{Tr}_{B^{(n_1, n_2)}} [\mathcal{L}'(t)\mathcal{G}(t,\tau)\mathcal{L}'(\tau)\mathcal{G}^\dagger(t,\tau)\rho_T(t)]. \quad (4)$$

Here, $\rho^{(n_1, n_2)}(t) = \text{Tr}_{B^{(n_1, n_2)}}[\rho_T(t)]$, is the reduced density matrix of the central system conditioned by the electron numbers emitted from the source lead (n_1) and arrived at the drain lead (n_2) until time t .

To proceed, following Ref. 30, two physical considerations are further implemented: (i) Instead of the conventional Born approximation for the entire density matrix $\rho_T(t) \simeq \rho(t) \otimes \rho_B$, we propose the ansatz $\rho_T(t) \simeq \sum_{n_1, n_2} \rho^{(n_1, n_2)}(t) \otimes \rho_B^{(n_1, n_2)}$, where $\rho_B^{(n_1, n_2)}(t)$ is the density operator of the electron reservoirs associated with n_1 -electrons emitted from the source and n_2 -electrons entered the drain. The orthogonality between reservoirs states in different subspaces leads to the term selection from the entire density operator ρ_T . (ii) Due to the closed nature of the transport circuit, the extra electrons entered the drain will flow back into the source via the external circuit. Also the rapid relaxation processes in the reservoirs will quickly bring the reservoirs to local thermal equilibrium characterized by the chemical potentials. As a consequence, after the state selection procedure, the electron reservoirs density matrices $\rho^{(n_1, n_2)}$ should be replaced by $\rho_B^{(0)}$.

Further use of the Markov-Redfield approximation

leads Eq.(4) to an explicit form:

$$\begin{aligned}\dot{\rho}^{(n_1, n_2)} &= -i\mathcal{L}\rho^{(n_1, n_2)} - \frac{1}{2}\mathcal{R}_1\rho^{(n_1, n_2)}, \quad (5a) \\ \mathcal{R}_1\rho^{(n_1, n_2)} &= \sum_j [d_j^\dagger A_j^{(-)} \rho^{(n_1, n_2)} + \rho^{(n_1, n_2)} A_j^{(+)} d_j^\dagger \\ &\quad - A_{Lj}^{(-)} \rho^{(n_1-1, n_2)} d_j^\dagger - d_j^\dagger \rho^{(n_1+1, n_2)} A_{Lj}^{(+)} \\ &\quad - A_{Rj}^{(-)} \rho^{(n_1, n_2-1)} d_j^\dagger - d_j^\dagger \rho^{(n_1, n_2+1)} A_{Rj}^{(+)}] + \text{H.c.} \quad (5b)\end{aligned}$$

Here $A_{\alpha j}^{(+)} = \sum_i \tilde{C}_{\alpha ij}^{(+)} (+\mathcal{L}) d_i$, $A_{\alpha j}^{(-)} = \sum_i \tilde{C}_{\alpha ji}^{(-)} (-\mathcal{L}) d_i$, and $A_j^{(\pm)} = \sum_{\alpha=L,R} A_{\alpha j}^{(\pm)}$. The spectral functions are defined in terms of the Fourier transform of the reservoir correlation functions, i.e., $\tilde{C}_{\alpha ij}^{(\pm)}(\pm\mathcal{L}) = \int_{-\infty}^{\infty} dt C_{\alpha ij}^{(\pm)}(t) e^{\pm i\mathcal{L}t}$. The reservoir correlators read $\langle f_{\alpha i}^\dagger(t) f_{\alpha j}(\tau) \rangle = C_{\alpha ij}^{(+)}(t - \tau)$, and $\langle f_{\alpha i}(t) f_{\alpha j}^\dagger(\tau) \rangle = C_{\alpha ij}^{(-)}(t - \tau)$. Here $\langle \dots \rangle$ stands for $\text{Tr}_B[\dots \rho_B^{(0)}]$, with the usual meaning of thermal average. Obviously, $\langle F_i^\dagger(t) F_j(\tau) \rangle = C_{ij}^{(+)}(t - \tau) = \sum_{\alpha=L,R} C_{\alpha ij}^{(+)}(t - \tau)$, and $\langle F_i(t) F_j^\dagger(\tau) \rangle = C_{ij}^{(-)}(t - \tau) = \sum_{\alpha=L,R} C_{\alpha ij}^{(-)}(t - \tau)$. For the sake of brevity, the explicit expressions of the reservoir correlation functions, the corresponding spectral functions, and $A_j^{(\pm)}$ are ignored here, and are presented alternatively in Appendix A.

At this stage, it is worth making a few remarks as follows: (i) The above particle-number-resolved master equation is applicable to finite temperatures, which is an extension of Gurvitz's approach [27]. (ii) The second-order cumulant expansion of H' restricts the applicability to the regime of sequential tunneling. However, generalization to higher order expansion of H' [36, 37] and self-consistent corrections[38] are possible. The corresponding FCS version is an interesting subject for future work. (iii) The above (n_1, n_2) -resolved master equation generalizes the result in Ref. 30, for electron counting from at one junction to at two junctions. Further generalization to multi-terminal setup is straightforward, following precisely the same treatment. (iv) The connection of the particle-number-resolved density matrix with the distribution function of FCS is obvious, i.e., $P(n_1, n_2, t) = \text{Tr}[\rho(t)^{(n_1, n_2)}]$, where the trace is over the central system states. From this distribution function, all orders of cumulants of transmission electrons can be calculated.

In practice, instead of obtaining the distribution function from the solution of the particle-number-resolved master equation, a more efficient method is the cumulant generating function (CGF) technique. In the following study, we only consider single counting statistics. That is, we only keep n_2 , after making summation over n_1 . Multiple counting statistics in multi-terminal setup follows the same technique.

Mathematically, the CGF is introduced as

$$e^{-F(\chi)} = \sum_n P(n, t) e^{in\chi}. \quad (6)$$

Here χ corresponds to the so-called counting field. Based on the CGF, the k th cumulant reads $C_k = -(-i\partial_\chi)^k F(\chi)|_{\chi=0}$. For instance, the first two cumulants give rise to the mean value of the transmitted electron numbers $C_1 = \bar{n}$, and the variance $C_2 = \overline{n^2} - \bar{n}^2$; the third cumulant (skewness), $C_3 = \overline{(n - \bar{n})^3}$, characterizes the asymmetry of the distribution. Here, $\overline{(\dots)} = \sum_n (\dots) P(n, t)$. Moreover, the cumulants are straightforwardly related to the transport characteristics, e.g., the average current by $I = eC_1/t$, and the zero-frequency shot noise by $S = 2e^2 C_2/t$. The Fano factor is defined as $F = C_2/C_1$, which represents the amplitude of current fluctuations, with $F > 1$ indicating a super-Poisson fluctuation, and $F < 1$ a sub-Poisson process.

The generating function can be calculated as follows. Define $S(\chi, t) = \sum_n \rho^{(n)}(t) e^{in\chi}$. Obviously, $e^{-F(\chi)} = \text{Tr}[S(\chi, t)]$. Let us reexpress the particle-number-resolved master equation formally as

$$\dot{\rho}^{(n)} = A\rho^{(n)} + C\rho^{(n+1)} + D\rho^{(n-1)}, \quad (7)$$

then $S(\chi, t)$ satisfies

$$\dot{S} = AS + e^{-i\chi} CS + e^{i\chi} DS \equiv \mathcal{L}_\chi S. \quad (8)$$

The formal solution reads $S(\chi, t) = e^{\mathcal{L}_\chi t} S(\chi, 0)$. In the low frequency limit, the counting time is much longer than the time of tunneling through the system. One can prove [20, 31, 34, 35], that $F(\chi) = -\lambda_1(\chi)t$, where $\lambda_1(\chi)$ is the eigenvalue of \mathcal{L}_χ , and satisfies the condition $\lambda_1(\chi) \mid_{\chi \rightarrow 0} \rightarrow 0$.

FCS Analysis

We now turn to the specific system under study. In the strong Coulomb blockade regime and at zero temperature, the matrix element form of the particle-number-resolved master equation reads

$$\begin{aligned}\dot{\rho}_{00}^{(n_2)} &= -2\Gamma_L \rho_{00}^{(n_2)} + \Gamma_R (\rho_{11}^{(n_2-1)} + \rho_{22}^{(n_2-1)}) \\ &\quad + \eta \Gamma_R (\rho_{12}^{(n_2-1)} + \rho_{21}^{(n_2-1)}), \quad (9a)\end{aligned}$$

$$\dot{\rho}_{11}^{(n_2)} = \Gamma_L \rho_{00}^{(n_2)} - \Gamma_R \rho_{11}^{(n_2)} - \eta \frac{\Gamma_R}{2} (\rho_{12}^{(n_2)} + \rho_{21}^{(n_2)}), \quad (9b)$$

$$\dot{\rho}_{22}^{(n_2)} = \Gamma_L \rho_{00}^{(n_2)} - \Gamma_R \rho_{22}^{(n_2)} - \eta \frac{\Gamma_R}{2} (\rho_{12}^{(n_2)} + \rho_{21}^{(n_2)}), \quad (9c)$$

$$\begin{aligned}\dot{\rho}_{12}^{(n_2)} &= i\delta\epsilon \rho_{12}^{(n_2)} + \Gamma_L \rho_{00}^{(n_2)} - \Gamma_R \rho_{12}^{(n_2)} \\ &\quad - \eta \frac{\Gamma_R}{2} (\rho_{11}^{(n_2)} + \rho_{22}^{(n_2)}). \quad (9d)\end{aligned}$$

Here we have summed n_1 and remained only n_2 , indicating the mere study of FCS of the electrons entered the drain reservoir. For clarity, we have denoted the level spacing by $\delta\epsilon = E_2 - E_1$, and choose the reference of zero energy such that $E_2 = \delta\epsilon/2$, and $E_1 = -\delta\epsilon/2$. In the derivation of Eqs. (9), we assumed that $E_{1,2}$ are inside the window of bias voltage, i.e., $\mu_L > E_{1,2} > \mu_R$, and

U is infinite. In Ref. 21 the same master equation was derived by a wavefunction approach.

Performing a discrete Fourier transformation $\sum_{n_2} e^{in_2\chi}$ to Eqs.(9), we obtain

$$\mathcal{L}_\chi = \begin{pmatrix} -2\Gamma_L & \Gamma_R e^{i\chi} & \Gamma_R e^{i\chi} & \eta\Gamma_R e^{i\chi} & \eta\Gamma_R e^{i\chi} \\ \Gamma_L & -\Gamma_R & 0 & -\eta\frac{\Gamma_R}{2} & -\eta\frac{\Gamma_R}{2} \\ \Gamma_L & 0 & -\Gamma_R & -\eta\frac{\Gamma_R}{2} & -\eta\frac{\Gamma_R}{2} \\ \Gamma_L & -\eta\frac{\Gamma_R}{2} & -\eta\frac{\Gamma_R}{2} & i\delta\epsilon - \Gamma_R & 0 \\ \Gamma_L & -\eta\frac{\Gamma_R}{2} & -\eta\frac{\Gamma_R}{2} & 0 & -i\delta\epsilon - \Gamma_R \end{pmatrix} \quad (10)$$

According to the definition of the cumulants we can express $\lambda_1(\chi)$ as

$$\lambda_1(\chi) = \frac{1}{t} \sum_{k=1}^{\infty} C_k \frac{(i\chi)^k}{k!}. \quad (11)$$

Then insert the above expansion into $|\lambda_1(\chi)I - \mathcal{L}_\chi| = 0$, and expand this determinant in series of $(i\chi)^k$. Since the value of $i\chi$ is arbitrary we can obtain C_k by setting the coefficients of $(i\chi)^k$ equal to zero and solving them sequentially [20]. Analytic expressions of the first two cumulants are accordingly obtained as

$$C_1 = \frac{2\Gamma_L\Gamma_R\delta\epsilon^2}{2\Gamma_L(\delta\epsilon^2 - (\eta-1)\Gamma_R^2) + \Gamma_R\delta\epsilon^2}, \quad (12a)$$

$$C_2 = \frac{\delta\epsilon^4\Gamma_R^2 + 4\Gamma_L^2[\delta\epsilon^4 + 2\delta\epsilon^2\eta\Gamma_R^2 + (\eta-1)^2\Gamma_R^4]}{[2\Gamma_L(\delta\epsilon^2 - (\eta-1)\Gamma_R^2) + \Gamma_R\delta\epsilon^2]^3} \times 2\Gamma_L\Gamma_R\delta\epsilon^2. \quad (12b)$$

while the higher order cumulants can be instead carried out numerically, to avoid their lengthy expressions.

In Fig. 1 the first three cumulants of transport current are displayed. It is of interest to note that in the Coulomb-blockade regime a super-Poisson noise is developed by the *constructive interference* between the two paths (i.e. $\eta = +1$). This is clearly shown by the solid curve in Fig. 1(a). With the increase of the coupling asymmetry (i.e. $\alpha = \Gamma_R/\Gamma_L$), the super-Poisson feature will be more evident. In contrast, for destructive interference ($\eta = -1$), the current fluctuation is sub-Poissonian, as plotted by the dashed curve in Fig. 1(a).

Another intriguing finding is that the super- and sub-Poisson characteristics are associated with different behaviors of the skewness C_3/C_1 , as shown in Fig. 1(b). For destructive interference, the skewness is approximately zero, meanwhile for constructive interference, transition of the skewness from (small) positive to (large) negative values takes place, by increasing the coupling asymmetry (α). As is well known for photon counting statistics in quantum optics, the skewness (both its magnitude and sign) provides further information for the counting statistics, beyond the second order cumulant. As a comparison, the results of non-interacting system are plotted in Fig. 1(c) and (d), where neither the super-Poisson noise nor the negative skewness is found.

To understand better the above super-Poisson behavior, below we present an analysis in terms of *fast-and-slow* transport channels. Let us introduce an

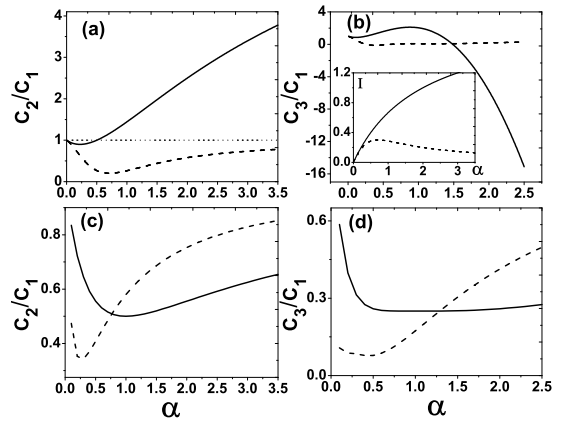


FIG. 1: First three cumulants of the zero-frequency current fluctuations. The solid and dashed curves display the results for constructive ($\eta = 1$) and destructive ($\eta = -1$) interferences, respectively. The variable $\alpha = \Gamma_R/\Gamma_L$ characterizes the asymmetry of dot-state couplings to the left and right electrodes. (a) and (b) show the Fano factor and skewness for strong Coulomb blockade system, while (c) and (d) for system allowing double occupancy, i.e., $U = 0.0$, as a comparison. Inset of (b) plots the average current $I = eC_1/t$, with the convention $e = 1$. In the calculation $\Gamma_L = 1.0\delta\epsilon$ was assumed.

alternative representation for the double dot states, with the corresponding electronic operators $f_1 = (\Omega_L d_1 + \Omega_R d_2)/\sqrt{\Omega_L^2 + \Omega_R^2}$, and $f_2 = (\Omega_L d_2 - \Omega_R d_1)/\sqrt{\Omega_L^2 + \Omega_R^2}$, as well as the state energies $E_{1/2} = \mp\frac{\delta\epsilon}{2}$. In such representation the entire Hamiltonian is reexpressed as

$$H = \tilde{E}_1 f_1^\dagger f_1 + \tilde{E}_2 f_2^\dagger f_2 + \gamma(f_1^\dagger f_2 + f_2^\dagger f_1) + \sum_k [\tilde{\Omega}_{1L} f_1^\dagger a_{Lk} + \tilde{\Omega}_{1R} f_1^\dagger a_{Rk} + \text{H.c.}] + \sum_k [\tilde{\Omega}_{2L} f_2^\dagger a_{Lk} + \tilde{\Omega}_{2R} f_2^\dagger a_{Rk} + \text{H.c.}]. \quad (13)$$

Note that the strong Coulomb blockade, rather than being explicitly described in this Hamiltonian, is reflected alternatively by the single occupation of the two dot states. For the sake of brevity, explicit expressions for the coupling between the new dot states, and their couplings to the electrodes are presented in Appendix B.

In the new states representation, the formation of the fast-and-slow transport channels is demonstrated in Fig. 2: (i) for constructive interference ($\eta = +1$), increasing $\alpha = \Gamma_R/\Gamma_L$ can lead to $\Gamma_{1L} > \Gamma_{2L}$, and $\Gamma_{1R} > > \Gamma_{2R}$; (ii) for destructive interference ($\eta = -1$), however, increasing $\alpha = \Gamma_R/\Gamma_L$ leads to $\Gamma_{1L} > \Gamma_{2L}$, but $\Gamma_{2R} > > \Gamma_{1R}$. Obviously, in the former case, an effective fast-and-slow transport channels are evaluated, but *can not* in the second case. Such fast-and-slow transport channels will lead to

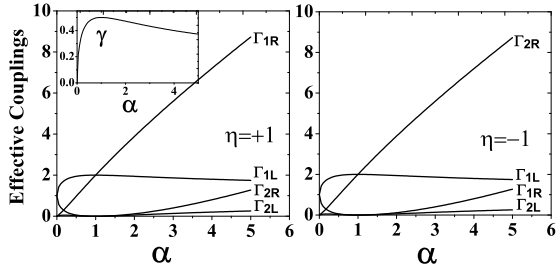


FIG. 2: Effective couplings of the dot states to the electrodes in the transformed state representation. It is found that effective fast-and-slow transport channels are evaluated for the constructive interference ($\eta = 1$), which is contrasted remarkably with the destructive interference ($\eta = -1$). Inset: effective coupling between the transformed dot states. Parameters $\alpha = \Gamma_R/\Gamma_L$, and $\Gamma_L = \delta\epsilon = 1.0$.

bunching behavior, and result in the super-Poisson noise [12, 13, 14, 15].

Decoherence Effect

To illustrate the decoherence effect, we consider dephasing between the two interfering paths, which is described by including the matrix element form of the following Lindblad-type terms

$$L_{\phi i} \rho^{(n_2)} L_{\phi i}^\dagger - \frac{1}{2} L_{\phi i}^\dagger L_{\phi i} \rho^{(n_2)} - \frac{1}{2} \rho^{(n_2)} L_{\phi i}^\dagger L_{\phi i}$$

into Eq.(9), where the jump operators $L_{\phi 1} = \sqrt{\Gamma_d}|1\rangle\langle 1|$, and $L_{\phi 2} = \sqrt{\Gamma_d}|2\rangle\langle 2|$. The effects of decoherence on the first three cumulants are shown in Fig. 3, where the solid and dashed curves correspond to the constructive ($\eta = 1$) and destructive ($\eta = -1$) interferences, respectively. Interestingly, for the constructively interfering transport ($\eta = 1$), dephasing does not influence the transport current, see the solid line in Fig. 3(a). This is in remarkable contrast with the result of double-slit optical interference, where the constructively interfering intensity is four times of the intensity of the individual path (slit), while the non-interfering intensity is simply two times of the single-slit intensity. This essential difference is originated from the multiple forward-and-backward scattering between the dot states and the electrodes in the case of electron transport. However, also for $\eta = 1$, the second and third cumulants (i.e. C_2 and C_3) sensitively depend on the dephasing strength. In particular, dephasing would cause a transition from super-Poisson to sub-Poisson processes, meanwhile the skewness (C_3) changes from negative value to zero. The present analysis clearly shows that the super-Poisson current fluctuation is a consequence of the constructive interference. For destructively interfering transport ($\eta = -1$), the almost

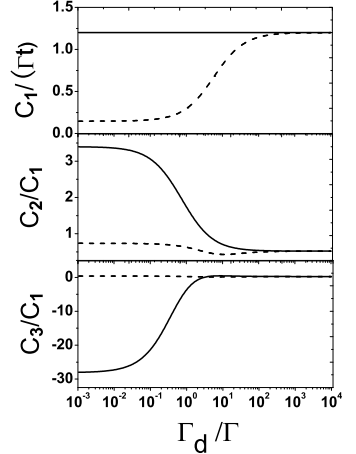


FIG. 3: Dephasing effects on the first three cumulants, which show a continuous transition from quantum interfering to classical non-interfering transports. The solid and dashed curves display results for the constructive ($\eta = 1$) and destructive ($\eta = -1$) interferences, respectively. Parameters $\alpha = \Gamma_R/\Gamma_L = 3.0$, and $\Gamma_L = \delta\epsilon = \Gamma$.

vanished transport current will be restored by dephasing, whereas the shot noise and skewness approximately do not change with dephasing.

Conclusion

To summarize, we have presented a FCS study for transport through a mesoscopic Coulomb blockade system with two identical transport channels. The FCS analysis showed that the shot noise and skewness are more sensitive than the average current to the underlying quantum interference. In particular, the average current cannot distinguish the quantum constructive interference from the classical non-interference, while the shot noise and skewness can fulfill that task. In the regime of quantum constructive interference, the interesting super-Poisson shot noise was found, and was understood in terms of an effective fast-and-slow channel picture via state-representation transformation. Dephasing effect has also been carried out to display the continuous transition of the first three cumulants from quantum interfering to classical non-interfering transports. Experiments within current technology are capable of examining the predictions of this work.

Methodologically, the present work extended the orthodox FCS approach in strong Coulomb-blockade systems [31]. The present approach can not only account for the many-body Coulomb interaction, but also handle the internal quantum coherence. This advantage allows for a wider range of applications.

Acknowledgments. This work was supported by the National Natural Science Foundation of China under grant No. 60425412 and No. 90503013, and the Research Grants Council of the Hong Kong Government.

APPENDIX A

In this appendix we present the explicit expressions of the spectral functions in Eq. (5) in the main text. For noninteracting electrodes and under the wide-band approximation, the reservoir correlation functions simply read

$$C_{Lij}^{(\pm)}(t-\tau) = g_L \Omega_L^2 \int d\varepsilon_{Lk} e^{\pm i\varepsilon_{Lk}(t-\tau)} n_L^{(\pm)}(\varepsilon_{Lk}), \quad (\text{A1a})$$

$$C_{Rii}^{(\pm)}(t-\tau) = g_R \Omega_R^2 \int d\varepsilon_{Rk} e^{\pm i\varepsilon_{Rk}(t-\tau)} n_R^{(\pm)}(\varepsilon_{Rk}), \quad (\text{A1b})$$

$$\begin{aligned} C_{R12}^{(\pm)}(t-\tau) &= \eta g_R \Omega_R^2 \int d\varepsilon_{Rk} e^{\pm i\varepsilon_{Rk}(t-\tau)} n_R^{(\pm)}(\varepsilon_{Rk}) \\ &= C_{R21}^{(\pm)}(t-\tau) \end{aligned} \quad (\text{A1c})$$

Here, the indices i and j denote the dot-states $|1\rangle$ and $|2\rangle$. Since the two dot-states are almost degenerate in energy and are equally coupled to the electrodes, in the above we have assumed that $\Omega_{i\alpha}\Omega_{j\alpha}^* = \Omega_{i\alpha}^*\Omega_{j\alpha} = \Omega_\alpha^2$. Note that an exception is $\Omega_{1R}^*\Omega_{2R} = \Omega_{2R}^*\Omega_{1R} = \eta\Omega_R^2$, where $\eta = \pm 1$ is the relative phase factor. This is because we have attributed the phase difference to the coupling amplitudes with the right electrodes. The electron and hole occupation functions are introduced, respectively, as $n_\alpha^{(+)}(\varepsilon_{\alpha k}) = n_\alpha(\varepsilon_{\alpha k})$, and $n_\alpha^{(-)}(\varepsilon_{\alpha k}) = 1 - n_\alpha(\varepsilon_{\alpha k})$, with $n_\alpha(\varepsilon_{\alpha k})$ the Fermi function. Fourier transformation of Eq. (A1) gives the spectral functions:

$$\tilde{C}_{Lij}^{(\pm)}(\omega) = \Gamma_L n_L^{(\pm)}(\mp\omega), \quad (\text{A2a})$$

$$\tilde{C}_{Rii}^{(\pm)}(\omega) = \Gamma_R n_R^{(\pm)}(\mp\omega), \quad (\text{A2b})$$

$$\tilde{C}_{R12}^{(\pm)}(\omega) = \tilde{C}_{R21}^{(\pm)}(\omega) = \eta\Gamma_R n_R^{(\pm)}(\mp\omega), \quad (\text{A2c})$$

where $\Gamma_\alpha = 2\pi g_\alpha \Omega_\alpha^2$.

Furthermore, using $\mathcal{L}d_j = -(E_j + Un_{\bar{j}})d_j$, the operators $A_{\alpha j}^{(\pm)}$ in Eq. (5), which is defined by $A_{\alpha j}^{(+)} = \sum_i \tilde{C}_{\alpha ij}^{(+)}(\mathcal{L})d_i$, $A_{\alpha j}^{(-)} = \sum_i \tilde{C}_{\alpha ji}^{(-)}(-\mathcal{L})d_i$, are accordingly obtained as

$$A_{\alpha j}^{(+)} = \sum_i \tilde{C}_{\alpha ij}^{(+)}[-(E_i + Un_{\bar{i}})]d_i, \quad (\text{A3a})$$

$$A_{\alpha j}^{(-)} = \sum_i \tilde{C}_{\alpha ji}^{(-)}[(E_i + Un_{\bar{i}})]d_i. \quad (\text{A3b})$$

Here the index \bar{i} simply means differing from i , i.e., $\bar{i} = 2$ if $i = 1$, and vice versa.

APPENDIX B

Via the transformation of state-representation as described in the main text, the energy levels of the transformed dot-states and their effective coupling strength read

$$\begin{aligned} \tilde{E}_1 &= \frac{\delta\epsilon}{2} \frac{\Omega_R^2 - \Omega_L^2}{\Omega_L^2 + \Omega_R^2}, \\ \tilde{E}_2 &= \frac{\delta\epsilon}{2} \frac{\Omega_L^2 - \Omega_R^2}{\Omega_L^2 + \Omega_R^2}, \\ \gamma &= \delta\epsilon \frac{\Omega_L\Omega_R}{\Omega_L^2 + \Omega_R^2}. \end{aligned} \quad (\text{B1})$$

Simple algebra also gives rise to the effective coupling strengths of the dot-states with the electrodes:

$$\begin{aligned} \tilde{\Omega}_{1L} &= \frac{\Omega_{1L}}{\sqrt{\Omega_L^2 + \Omega_R^2}}(\Omega_L + \Omega_R), \\ \tilde{\Omega}_{1R} &= \frac{\Omega_{2R}}{\sqrt{\Omega_L^2 + \Omega_R^2}}(\eta\Omega_L + \Omega_R), \\ \tilde{\Omega}_{2L} &= \frac{\Omega_{1L}}{\sqrt{\Omega_L^2 + \Omega_R^2}}(\Omega_L - \Omega_R), \\ \tilde{\Omega}_{2R} &= \frac{\Omega_{2R}}{\sqrt{\Omega_L^2 + \Omega_R^2}}(\Omega_L - \eta\Omega_R). \end{aligned} \quad (\text{B2})$$

More transparently, for $\eta = 1$, the corresponding tunneling rates read

$$\begin{aligned} \Gamma_{1L} &= \frac{\Gamma_L(\Gamma_L + \Gamma_R + 2\sqrt{\Gamma_L\Gamma_R})}{\Gamma_L + \Gamma_R}, \\ \Gamma_{1R} &= \frac{\Gamma_R(\Gamma_L + \Gamma_R + 2\sqrt{\Gamma_L\Gamma_R})}{\Gamma_L + \Gamma_R}, \\ \Gamma_{2L} &= \frac{\Gamma_L(\Gamma_L + \Gamma_R - 2\sqrt{\Gamma_L\Gamma_R})}{\Gamma_L + \Gamma_R}, \\ \Gamma_{2R} &= \frac{\Gamma_R(\Gamma_L + \Gamma_R - 2\sqrt{\Gamma_L\Gamma_R})}{\Gamma_L + \Gamma_R}, \end{aligned} \quad (\text{B3})$$

and for $\eta = -1$, they are

$$\begin{aligned} \Gamma_{1L} &= \frac{\Gamma_L(\Gamma_L + \Gamma_R + 2\sqrt{\Gamma_L\Gamma_R})}{\Gamma_L + \Gamma_R}, \\ \Gamma_{1R} &= \frac{\Gamma_R(\Gamma_L + \Gamma_R - 2\sqrt{\Gamma_L\Gamma_R})}{\Gamma_L + \Gamma_R}, \\ \Gamma_{2L} &= \frac{\Gamma_L(\Gamma_L + \Gamma_R - 2\sqrt{\Gamma_L\Gamma_R})}{\Gamma_L + \Gamma_R}, \\ \Gamma_{2R} &= \frac{\Gamma_R(\Gamma_L + \Gamma_R + 2\sqrt{\Gamma_L\Gamma_R})}{\Gamma_L + \Gamma_R}. \end{aligned} \quad (\text{B4})$$

[1] Ya. M. Blanter and M. Büttiker, Phys. Rep. **336**, 1 (2000); *Quantum Noise in Mesoscopic Physics*, edited by Yu. V. Nazarov (Kluwer, Dordrecht, 2003).

[2] L. S. Levitov, H. W. Lee, and G. B. Lesovik, J. Math. Phys. **37**, 4845 (1996).

[3] V. K. Khlus, Sov. Phys. JETP **66**, 1243 (1987).

[4] S. Gustavsson, R. Leturcq, B. Simović, R. Schleser, T. Ihn, P. Studerus, K. Ensslin, D. C. Driscoll, and A. C. Gossard, Phys. Rev. Lett. **96**, 076605 (2006); T. Fujisawa, T. Hayashi, R. Tomita, and Y. Hirayama, Science **312**, 1634 (2006).

[5] M. Büttiker, Phys. Rev. B **46**, 12485 (1992); M. Henny, S. Oberholzer, C. Strunk, and C. Schönenberger, Science **284**, 296 (1999); W. D. Oliver, Jungsang Kim, Robert C. Liu, Y. Yamamoto, Science **284**, 299 (1999).

[6] M. J. M. de Jong and C. W. J. Beenakker, Phys. Rev. B **49**, 16070 (1994); B. A. Muzykantskii and D. E. Khmel'nitskii, Phys. Rev. B **50**, 3982 (1994); W. Belzig and Yu. V. Nazarov, Phys. Rev. Lett. **87**, 067006 (2001).

[7] A. A. Kozhevnikov, R. J. Schoelkopf, and D. E. Prober, Phys. Rev. Lett. **84**, 3398 (2000); X. Jehl, M. Sanquer, R. Calemczuk, and D. Mailly, Nature **405**, 50 (2000).

[8] T. Hoss, C. Strunk, T. Nussbaumer, R. Huber, U. Staufer, and C. Schönenberger, Phys. Rev. B **62**, 4079 (2000); R. Cron, M. F. Goffman, D. Esteve, and C. Urbina, Phys. Rev. Lett. **86**, 4104 (2001).

[9] J. C. Cuevas, A. Martín-Rodero, and A. Levy Yeyati, Phys. Rev. Lett. **82**, 4086 (1999); Y. Naveh and D. V. Averin, Phys. Rev. Lett. **82**, 4090 (1999).

[10] W. Belzig and Yu. V. Nazarov, Phys. Rev. Lett. **87**, 197006 (2001).

[11] G. Johansson, P. Samuelsson, and Åke Ingerman, Phys. Rev. Lett. **91**, 187002 (2003); S. Pilgram and P. Samuelsson, Phys. Rev. Lett. **94**, 086806 (2005).

[12] S. S. Safonov, A. K. Savchenko, D. A. Bagrets, O. N. Jouravlev, Yu. V. Nazarov, E. H. Linfield, and D. A. Ritchie, Phys. Rev. Lett. **91**, 136801 (2003).

[13] A. Thielmann, M. H. Hettler, J. Kö nig, and G. Schön, Phys. Rev. B **71**, 045341 (2005); J. Aghassi, A. Thielmann, M. H. Hettler, and G. Schön, Phys. Rev. B **73**, 195323 (2006).

[14] W. Belzig, Phys. Rev. B **71**, 161301(R) (2004).

[15] B. R. Bulka, Phys. Rev. B **62**, 1186 (2000); A. Cottet, W. Belzig, and C. Bruder, Phys. Rev. Lett. **92**, 206801 (2004).

[16] G. Iannaccone, G. Lombardi, M. Macucci, and B. Pellegrini, Phys. Rev. Lett. **80**, 1054 (1998); A. N. Jordan and E. V. Sukhorukov, Phys. Rev. Lett. **93**, 260604 (2004); ibid. **94**, 059901(E) (2005).

[17] E. V. Sukhorukov, G. Burkard, and D. Loss, Phys. Rev. B **63**, 125315 (2001); A. Thielmann, M. H. Hettler, J. König, and G. Schön, Phys. Rev. Lett. **95**, 146806 (2005).

[18] E. Onac, F. Balestro, B. Trauzettel, C. F. J. Lodewijk, and L. P. Kouwenhoven, Phys. Rev. Lett. **96**, 026803 (2006).

[19] Ya. M. Blanter, O. Usmani, and Yu. V. Nazarov, Phys. Rev. Lett. **93**, 136802 (2004); ibid. **94**, 049904(E) (2005); T. Novotny, A. Donarini, C. Flindt, and A-P. Jauho, Phys. Rev. Lett. **92**, 248302 (2004); J. Koch and Felix von Oppen, Phys. Rev. Lett. **94**, 206804 (2005).

[20] C. W. Groth, B. Michaelis, and C. W. J. Beenakker, Phys. Rev. B **74**, 125315 (2006).

[21] S. A. Gurvitz, IEEE Transactions on Nanotechnology, **4**, 45 (2005).

[22] A. W. Holleitner, C. R. Decker, H. Qin, K. Eberl, and R. H. Blick, Phys. Rev. Lett. **87**, 256802 (2001); A. W. Holleitner, R. H. Blick, A. K. Hüttel, K. Eberl, and J. P. Kotthaus, Science **297**, 70 (2002).

[23] M. Sigrist, T. Ihn, K. Ensslin, D. Loss, M. Reinwald, and W. Wegscheider, Phys. Rev. Lett. **96**, 036804 (2006).

[24] G. Hackenbroich, Phys. Rep. **343**, 463 (2001).

[25] A. Yacoby, M. Heiblum, D. Mahalu, and H. Shtrikman, Phys. Rev. Lett. **74**, 4047 (1995); R. Schuster, E. Buks, M. Heiblum, D. Mahalu, V. Umansky, and H. Shtrikman, Nature **385**, 417 (1997); M. Avinun-Kalish, M. Heiblum, O. Zarchin, D. Mahalu, and V. Umansky, Nature **436**, 529 (2005).

[26] O. Entin-Wohlman, A. Aharony, Y. Imry, Y. Levinson, and A. Schiller, Phys. Rev. Lett. **88**, 166801 (2002); A. Aharony, O. Entin-Wohlman, B. I. Halperin, and Y. Imry, Phys. Rev. B **66**, 115311 (2002).

[27] S. A. Gurvitz and Ya. S. Prager, Phys. Rev. B **53**, 15932 (1996).

[28] Y. Makhlin, G. Schön, and A. Shnirman, Rev. Mod. Phys. **73**, 357 (2001).

[29] Xin-Qi Li, Ping Cui, and YiJing Yan, Phys. Rev. Lett. **94**, 066803 (2005).

[30] Xin-Qi Li, Jun-Yan Luo, Yong-Gang Yang, Ping Cui, and YiJing Yan, Phys. Rev. B **71**, 205304 (2005).

[31] D. A. Bagrets, Yu. V. Nazarov, Phys. Rev. B **67**, 085316 (2003).

[32] Yu. V. Nazarov, Ann. Phys. (Leipzig) **8**, SI-193 (1999), cond-mat/9908143; W. Belzig, *Quantum Noise*, edited by Yu. V. Nazarov and Ya. M. Blanter, cond-mat/0210125.

[33] Yu. V. Nazarov, *Quantum Dynamics of Submicron Structures*, eds. H. Cerdeira, B. Kramer, G. Schoen (Kluwer, 1995), p. 687; Yu. V. Nazarov and D. A. Bagrets, Phys. Rev. Lett. **88**, 196801 (2002).

[34] C. Flindt, T. Novotny, A. P. Jauho, Europhys. Lett., **69**, 475 (2005).

[35] G. Kießlich, P. Samuelsson, A. Wacker, E. Schöll, Phys. Rev. B **73**, 033312 (2006).

[36] Rui-Xue Xu, Ping Cui, Xin-Qi Li, Yan Mo, and YiJing Yan, J. Chem. Phys. **122**, 041103 (2005).

[37] Jinshuang Jin, Sven Welack, JunYan Luo, Xin-Qi Li, Ping Cui, Rui-Xue Xu, and YiJing Yan, cond-mat/0612137; Rui-Xue Xu, and YiJing Yan, cond-mat/0612649.

[38] Ping Cui, Xin-Qi Li, Jiushu Shao, and YiJing Yan, Phys. Lett. A **357**, 449 (2006).